$$\frac{\partial u'}{\partial x} + \frac{\partial w'}{\partial z} = 0 \qquad (A5)$$

$$-\frac{2}{\rho}\nabla p + \left(\frac{\mu_2 + \eta}{\sqrt{\eta\omega}}\right)\varphi \hat{k} - \frac{\mu_1}{\sqrt{\omega}} w' \frac{\partial V}{\partial z}\hat{j} - \frac{\mu}{\sqrt{\omega}} v \frac{\partial V}{\partial z}\hat{k}$$

$$= -\frac{2}{\rho}\nabla^2(v\hat{j} + u'\hat{i} + w'\hat{k}) \qquad (A6)$$

$$\frac{\mu_2 + \eta}{\sqrt{\eta\omega}} w' = -\frac{2}{\rho}\nabla^2\varphi \qquad (A7)$$

The natural boundary conditions at $z = 1$ are

$$\frac{2}{\rho}\frac{\partial \varphi}{\partial z} + \sqrt{\frac{\omega}{\eta}}\frac{\partial w'}{\partial z} = 0 \qquad (A8a)$$

$$\frac{\partial v}{\partial z} = 0 \qquad (A8b)$$

$$\sqrt{\frac{\omega}{\eta}}\frac{\partial \varphi}{\partial x} + \frac{2}{\rho}\frac{\partial u'}{\partial z} = 0 \qquad (A8c)$$

The Fourier decomposition proceeds as before, except that $K_y = 0$ and $K_x = K$. Equations (2.6) and (2.7) become

$$(D^2 - K^2)^3 w' + K^2 \left[\frac{(\mu_2 + \eta)^2}{\omega\eta} + \frac{\mu_1{}^2}{\omega}\right]\frac{\rho^2}{4} w' = 0 \qquad (A9)$$

$$K^2 p = (D^2 - K^2) D\, w' \qquad (A10)$$

Equations (2.8b) and (2.9) become

$$\varphi = \sum_{i=1}^{6} A_i \frac{\rho}{2}\frac{\mu_2 + \eta}{\sqrt{\omega\eta}} e^{im_i z} + A_7 e^{Kz} + A_8 e^{-Kz} \qquad (A11)$$

$$(\mu_2 + \eta)D\varphi =$$

$$-\frac{2}{\rho}\sqrt{\eta\omega}\left[2D^3 w' - K^2 D w' - \frac{1}{K^2} D^5 w'\right] \qquad (A12)$$

whereas (2.8a) remains the same. Instead of (2.10), Equations (A8b) and (A8c) become

$$D^2 w' + \frac{\rho}{2} K^2 \frac{\sqrt{\omega}}{\sqrt{\eta}} \varphi = 0 \qquad (A13)$$

The solution technique for ρ is the same as before, only the boundary conditions to use are (A13), (A12), (2.11) and (A8a), and a slightly modified (2.4b):

$$\frac{\partial w'}{\partial z}(0) = w'(0) = \varphi(0) = w'(1) = 0 \qquad (A14)$$

One point on the stability boundary, $Ra = 150$, $Re = 35$, was calculated using this technique. It was assumed that K and λ retain the same values as when $\omega = 1$. Although this was not verified the independence of λ_{opt} and K_{opt} was well established. The new stability point is at $Ma = 31.1$ (at $\omega = 2$ compared to $Ma = 22.2$ (at $\omega = 1$). While the stability boundary is raised significantly, note that it still falls below that for transverse disturbances.

Part III. Experiments

Convective instabilities in shear flow are studied experimentally in a horizontal concurrent two-phase flow channel. The convective instabilities are generated by interphase mass transfer between the two immiscible liquid phases. Schlieren photography perpendicular to the interface is used to record both the disturbance shape and its orientation. Three separate convective modes are studied: A. surface tension driven, B. buoyancy driven, and C. coactive buoyancy and surface tension driven. The disturbance structure of mode A appears as rings which oscillate in diameter as they are swept downstream. Streamwise oriented roll vortices also appear when flow conditions move the interface into a region of higher shear. Modes B and C are both characterized by streamwise oriented roll vortices with mode C having an additional fine structure.

SCOPE

Diffusive heat or mass transfer is often unstable with respect to convective instabilities. These instabilities can be from two possible sources. Most commonly, temperature or concentration variations cause differences in density. This may result in natural convection. Secondly, variations in temperature and concentration of an interface cause differences in surface tension and hence result in motion. While these two mechanisms cause many fascinating naturally occurring phenomena, they are also of great practical importance in industry. This importance arises from the manyfold enhancement of transport rates when convection is present.

Most interesting problems in this area, especially those of a practical sort, involve the presence of a primary shearing motion simultaneously occurring with heat or mass transfer. Unfortunately, most theoretical and experimental effort up until now has dealt with stagnant systems. In two previous papers (Gumerman and Homsy, 1974a, 1974b), we have dealt with theoretical aspects of the problem when shear is present. Specifically, criteria were developed to find if a system is stable or not. And, if the system is unstable, what orientation the disturbance will take.

This paper will deal with experiments concerning the effect of low Reynolds number shear on convective instabilities. The few previous experimental investigations in this area fall into two groups. In the first, enhancement

rates are measured. The second group deals with buoyancy instabilities in a one fluid system (no free interface). This paper deals with qualitative observations of disturbance orientation in a two fluid system. This problem is of practical interest since transport usually is across a deformable interface. Eventually, information on disturbance orientation may help in solving the nonlinear convective equations and allow transport rate predictions. For the present, however, we will simply compare results with predictions of Gumerman and Homsy (1974a, 1974b).

CONCLUSIONS AND SIGNIFICANCE

In the present work, immiscible fluid pairs were contacted in a horizontal flow channel. Convective instabilities developed downstream from the point of contact when a solute was dissolved in one of the phases. The resulting disturbances were recorded using schlieren photography.

There are three basic convective modes possible in this situation, as discussed by Berg and Morig (1969). That is the instability can be caused by, A. surface tension alone, with buoyancy stabilizing; B. buoyancy alone; or C. buoyancy and surface tension. Types B and C are called *unconfined convection* since the fluid disturbance motion may reach the horizontal boundaries of the apparatus. Type A is termed *confined convection* since the stable stratification will confine the fluid motion to the interface region.

Three different chemical systems were chosen for our study, one representing each of the above types of behavior. In each case a characteristic disturbance developed.

In both cases of unconfined convection we found a roll pattern developing, with the roll axes parallel to direction of flow. When surface tension was not destabilizing, the schlieren picture was clear and steady, with only several longitudinal lines present. When surface tension was also destabilizing, the image had an additional grainy time-dependent structure due to some unordered, small-scale disturbance.

In the case of confined convection an unexpected ring shaped pattern was present. These rings oscillated in size as they were swept downstream. A secondary longitudinal roll pattern developed only in cases of high flow rate or high relative flow rate between the two phases.

While the ring pattern observed for confined convection is unexplained, other observations are in qualitative agreement with previous predictions.

It is well known that interphase heat or mass transfer can cause spontaneous convection. Depending on the system, this convection is caused by two mechanisms acting individually or simultaneously. First, differences in concentration or temperature cause differences in density. When the direction of diffusive transport is such that low density fluid underlies fluid of a higher density, the system is unstable to buoyancy instabilities. Secondly, differences in temperature or concentration occurring at a fluid/fluid interface cause differences in the interfacial tension. These differences in tension can generate motion which is self-sustaining.

Excellent reviews of the vast amount of experimental work which has been done in this area include Berg et al. (1966), Sawistowski (1971), and Berg (1972). Most experimental work has dealt with systems that are stagnant except for the spontaneous secondary convection. This previous work is primarily of two types. The enhancement of transport rates caused by convection is measured in batch cells. Or, more commonly, the structure of the instability is studied by observing with some suitable visualization technique like schlieren photography.

There are only a few experimental works dealing with systems having a primary shearing motion. Maroudas and Sawistowski (1964) measured convective enhancement of overall mass transfer rates in the carbon tetrachloride-water system using propionic acid and phenol as solutes. Their experiments were done in both a wetted wall column and a horizontal contactor. The horizontal contactor was equipped with side windows and schlieren photography was used. Unfortunately, it is impossible to determine the disturbance orientation from pictures taken in the plane of the interface.

Both Clark and King (1970) and Brian et al. (1971) studied convective enhancement of desorption. In both cases volatile solutes were desorbed from water into nitrogen. The former study used a horizontal flow channel while the latter used a wetted wall column. Neither study included visualization techniques. Another purely quantitative study of convective enhancement was carried out by Bakker et al. (1967). Their study involved liquid-liquid extraction in a wetted wall column.

Some brief qualitative work was done by Linde and Schwarz (1964) in a horizontal concurrent flow channel of 2-cm square cross section. A 2% mixture of C_8-C_{16} sodium alkyl surfactants dissolved in isoamyl alcohol was contacted with water. This system is known to be unstable to interface driven disturbances. Schlieren pictures were taken perpendicular to the interface to record the convective structure while the surfactant was transferred. The structure was found to be flow rate dependent. At an interface velocity of 0.1 to 0.2 cm/s there were one or two large roll cells oriented parallel to the primary flow (that is, longitudinal rolls). Near the inlet the structure was chaotic. At interface velocities exceeding 1 cm/s, no convection was visible. At intermediate velocities, between 0.5 and 1 cm/s disturbances took on an unaligned form and oscillated rapidly while being swept downstream. The disturbances increased in size with decreasing velocity and there was a transition to longitudinal rolls at the lower flow rate. Experiments on otherwise stagnant pools of the same chemical system reveal both low (0.5 to 5 s^{-1}) and high (10 to 20 s^{-1}) frequency oscillation of disturbances.

There are a number of experimental works dealing with buoyancy instability alone in Couette flow (Brunt, 1951; Chandra, 1938; Benard and Avsec, 1938; Graham, 1933). In these works, a fluid layer between horizontal rigid walls (in relative motion) was heated from below. Phillips and Walker (1932) experimentally considered the related Poiseuille flow problem. These works clearly show the dominance of the longitudinal roll pattern when buoyancy instabilities are present in a one fluid layer.

This review makes clear that there is much yet to be learned from experiments concerning the effect of shear on convective instabilities. When the instability is driven by buoyancy, the disturbance appears to take the form of longitudinal rolls. This is verified for a fluid layer between rigid horizontal bounding surfaces but has not yet been verified for the case of two immiscible phases separated by a deformable interface. In addition, aside from the brief study by Linde and Schwarz (1964), no one has studied the disturbance structure when interface driven instabilities are present.

The present work is a qualitative study of convective disturbance structure when shear is present. Our purpose is two-fold. First, this study helps to fill the void in the literature just mentioned. That is, this work studies the effect of a deformable interface on buoyancy convection, and more importantly, it studies structure when surface driven instabilities are present. Secondly, we want to qualitatively compare experimental results with predictions of Parts I and II (Gumerman and Homsy, 1974a, 1974b).

Parts I and II are stability analyses for heat transfer induced convection in couette flow. Part I is a linear stability analysis for a two-phase system in which the interface is allowed to deform. Part II is an energy method stability analysis. In Part II the fluid mechanics of the upper phase is neglected and the interface is not allowed to deform (that is, it remains planar). There are several differences between these analyses and the experiments reported here. A stability analysis for mass transfer must include the effect of the Gibbs adsorption layer on the interface. As shown by Palmer and Berg (1972) and Brian and Ross (1972), the adsorption layer has a stabilizing effect. Its influence on disturbance orientation is unknown. In Parts I and II we assumed a linear temperature and velocity profile for simplicity. Experimentally this is difficult to achieve, especially for an initial study. However, in the case of the energy method used in Part II, results are known to be quite insensitive to the velocity profile.

In Parts I and II it was found that the disturbance will be a longitudinal roll, at least when the interfacial tension and density difference (between the fluids on either side of the interface) are sufficiently large. These conditions are met by the chemical systems used here.

In this study, a horizontal contactor was used to bring together two immiscible liquid phases, one of which contained a solute. Mass transfer caused the convective instabilities. A horizontal contactor was chosen rather than a wetted wall column because theoretical studies of convection usually have the gravity vector perpendicular to the interface. Unlike Maroudas and Sawistowski (1964), in this study the schlieren beam is perpendicular to the interface so that disturbance orientation can be observed.

The Reynolds number was held at low to moderate values in this study since the thrust of the work is to study the effect of shear on convection.

There are three main convection modes that must be considered, as pointed out by Berg and Morig (1969). Mode A is surface tension driven buoyancy stabilized. We will call this case confined convection since the disturbance is confined to the interface region due to the stabilizing density gradient. B. The density driven mode is unconfined in the sense that the disturbance will reach all the way to the upper and lower boundaries. C. The coactive buoyancy and surface tension driven regime will also be unconfined. It should be pointed out that in B and C, the buoyancy instability can arise in either one or both of the two phases.

APPARATUS AND PROCEDURE

Three chemical systems were chosen for this study. Each of the instability modes described by Berg and Morig (1969) is represented by one of the systems. The systems are:

A. Acetone transferring downwards from water to carbon tetrachloride. This system exhibits confined surface tension driven convection. Buoyancy is stabilizing in both phases.

B. Acetone transferring upward from carbon tetrachloride to water. In this case, the pair is unstable to buoyancy instabilities in both phases. No surface tension driven instabilities are expected.

C. Acetic acid transferring downward from isobutanol to water. This particular system will be unstable to both surface tension and buoyancy convection. The density gradient is unstable in both phases.

The systems described above were also used by Bakker et al. (1967) in their measurements of enhancement rates in stagnant systems.

The Sternling and Scriven (1959) criteria were used to judge whether the surface tension driven mode would be present in each case. It is, of course, a simple matter to predict if buoyancy instabilities occur by comparison of relative densities.

Figure 1 shows the flow channel used to contact the two liquid phases. The channel is made of stainless steel with Plexiglas windows and consists of three sections—a flow straightening section (14 cm long), an observation section (20 cm long), and an outlet section. The two phases are fed separately into flow straightening sections, the dense phase fed in from below and the less dense phase from above. The phases are separated from each other in this section by a thin bisecting shim. The shim tapers to a point 0.2 cm short of the observation windows. At this point the two phases meet and mass transfer begins. In both the observation section and straightening section (neglecting the separating shim) the flow area is 4 cm wide by 1 cm high.

The upper and lower surfaces of the observation section are Plexiglas windows. The schlieren beam (discussed below) is directed vertically downwards through these windows.

The two phases were withdrawn through a 0.2-cm high slot located midway in height between the upper and lower surface of the observation section. To prevent buildup of surfactant at the interface, an outlet section is attached to the weir. The interface drops into the outlet section and is withdrawn through the lower of the two outlet tubes.

A schematic of the entire flow loop is shown in Figure 2. The flow channel was fed from two reservoirs by pressurized dry nitrogen. The reservoirs, valves, tubing, and rotameters were made of stainless steel, glass, and teflon.

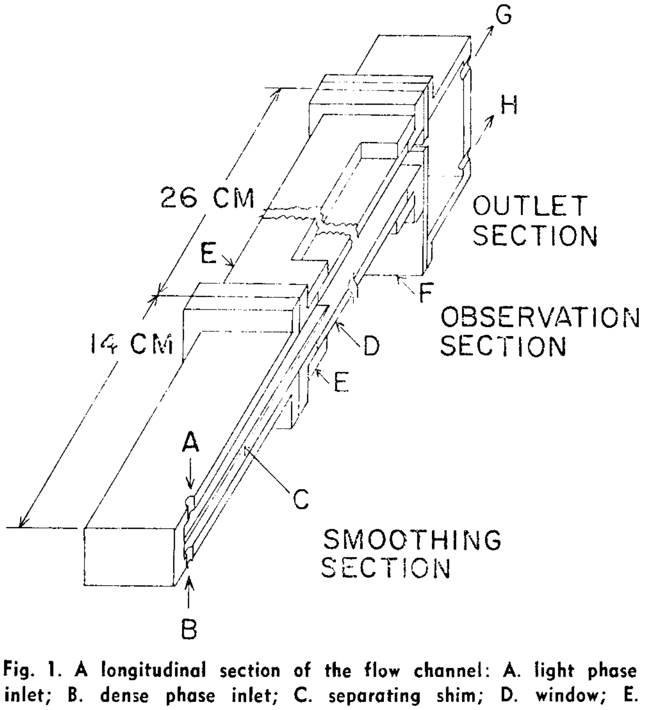

Fig. 1. A longitudinal section of the flow channel: A. light phase inlet; B. dense phase inlet; C. separating shim; D. window; E. window clamp; F. weir; G. light phase outlet; H. light and dense phase outlet.

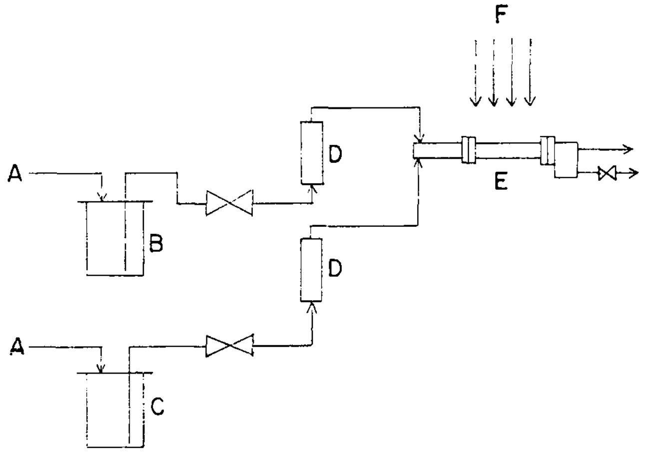

Fig. 2. Schematic of experimental equipment: A. Compressed nitrogen inlet; B. light phase reservoir; C. dense phase reservoir; D. rotameter; E. flow channel; F. schlieren field.

Schlieren photography is a common means of flow visualization in convection studies. The technique is described in Holder and North (1956) and elsewhere. The basic principle here is that differences in solute concentration cause differences in index of refraction. The parallel schlieren beam reveal index of refraction gradients perpendicular to the beam. So, in this case horizontal gradients of solute concentration are seen. The schlieren equipment used in this study is the same as that described in Berg et al. (1966). Here, a 16-mm ciné camera was used to record the structure and orientation of the instabilities.

In these experiments reagent grade chemicals were used. Solvents were reused in subsequent runs after distillation. Several times during the experiments the channel (excluding windows), tubing, and rotameters were cleaned with chromic acid. The experimental procedure consisted in contacting the two solvents overnight to ensure mutual saturation and temperature equilibration (24°C). They were then separated and put in their respective reservoirs. A predetermined amount of solute was mixed into the appropriate solvent and the reservoirs were sealed and pressurized. The flow rate was turned up high and the channel was tipped to-and-fro to remove air bubbles. The flow rate was then adjusted to its run value. When no further change in the schlieren image (in the camera viewfinder) was observed, pictures were taken. The knife edge was positioned to get the best contrast.

The best image was achieved using the following: aperature setting 2.2, shutter half closed, N.G. 90 filter, 12 frames/sec., and schlieren knife edge cutting off 2/3 of the light. Kodak Plus X reversal film was used. The camera used was a Bolex H16 Reflex with an Angenieux F. 12-120-mm zoom lens.

OBSERVATIONS

Surface Tension Driven Confined Convection

The system (A) water-carbon tetrachloride with acetone transferred downwards is susceptible to surface tension driven instabilities under the Sternling and Scriven (1959) criteria. It is stable in both phases to buoyancy instability. This system was observed at initial solute concentrations of 0.20, 0.30, and 0.60 molar and with volumetric flow rates ranging downwards from 60 ml/min $\left[\frac{26.7}{42.0}\right]$ for each phase. Here and in the following discussion the Reynolds number is in brackets. The Reynolds number of the upper phase is the upper number and that of the lower denser phase is the lower number. The Reynolds number is defined as

$$Re = \frac{\dot{V}}{W\nu}$$

where $\dot{V}$ is the volumetric flow rate and W is the width of the channel, 4 cm.

Quite surprisingly, the characteristic instability of this system is neither a longitudinal roll nor a transverse wave. Instead, we observed circular shaped disturbances that were swept along with the flow. At high solute concentrations the circles are more like explosions—they appear and steadily increase in diameter with time until they are indistinguishable. At low solute concentrations in the disturbances maintain their integrity and oscillate in size (diameter) at a frequency of $\sim 1\ s^{-1}$. This oscillation is clearly a flow induced effect—when the flow through the channel is stopped, the oscillation stops. Linde and Schwarz (1964) apparently observed a similar oscillatory pattern, but their system also had oscillating disturbances when stagnant.

The cell size observed here decreases when either the total volumetric flow rate through the channel increased, or the difference between the flow rates of the two phases increased. This latter case corresponds to a change in the relative depths of the two phases. Generally speaking, the density of cells decreases, and the cells elongate as the interface ages.

At the lowest solute concentration observed, when the difference in flow rates of the two phases was sufficiently large, faint longitudinal lines were observed in addition to the circular disturbances. Specifically, this was observed when the ratio of water to carbon tetrachloride (in ml/min.) was 30/50 $\left[\frac{13.3}{35.0}\right]$, 10/72 [4.4/50.4], and 70/8 $\left[\frac{31.1}{5.6}\right]$. Presumably the longitudinal roll pattern was due to a movement of the convecting interface region into a region of larger shear.

Figure 3 shows the typical appearance of the ring pattern. The initial acetone concentration is 0.20 molar, and the flow rates are 30 ml/min water, 30 ml/min carbon tetrachloride $\left[\frac{13.4}{21}\right]$. In these pictures the side walls of

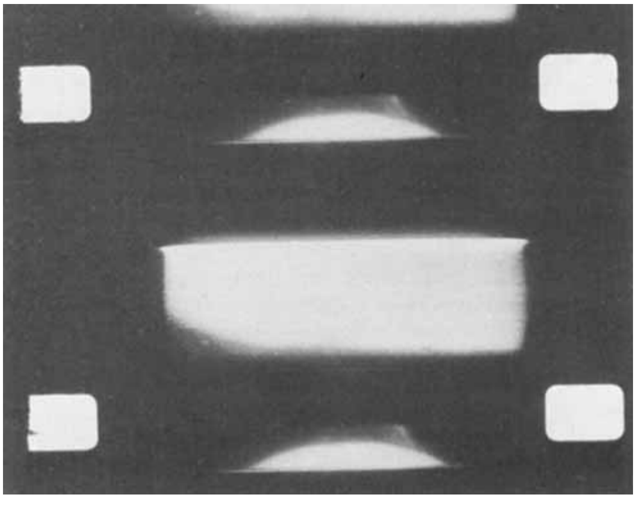

Fig. 3. Typical disturbance structure of combined buoyancy and surface tension driven flow. The solvent phases are isobutyl alcohol and water, the former at 50 ml/min. and the latter at 90 ml/min., $\left[\frac{4.5}{40}\right]$. The initial solute (acetic acid) concentration is 0.10 molar in the alcohol. Note both the longitudinal alignment and the equal spacing of the four rolls. The fourth longitudinal line is barely visible at the edge of the meniscus (bottom of picture).

the channel appear as black bands. The meniscus effect causes either a shaded or a bright area near the side walls.

Unconfined Buoyancy Driven Convection

The system (B) water-carbon tetrachloride with upward transfer of acetone is susceptible to buoyancy instabilities in both phases and stable to surface tension instabilities by the Sternling and Scriven (1959) criteria. Initial solute concentrations of 0.25 and 0.05 molar acetone were used, the former having a chaotic exploding type pattern at any flow rate. This was presumably due to highly supercritical conditions.

As expected, the disturbances at the lower solute concentration were longitudinal rolls. No disturbances had time to develop when the flow rate exceeded 10 ml/min. $\left[\frac{4.4}{7.0}\right]$ in each phase. A variety of longitudinal roll patterns appeared when one of the phases had zero net flow (and hence is recirculating), and the other phase flow rate was varied from 0-50 ml/min. $\left[\frac{22.2}{35.0}\right]$.

Figure 4 shows typical behavior for this mode. The initial concentration is 0.05 molar. The flow rates are zero water, and 18 ml/min. carbon tetrachloride $\left[\frac{0}{12.6}\right]$. A small drop of carbon tetrachloride on the upper window caused the black mark midchannel on this photograph.

Unconfined Coactive Buoyancy and Surface Tension Driven Convection

The system (C) isobutyl alcohol-water with acetic acid transferred downwards is susceptible to surface tension driven instability under the Sternling and Scriven criteria, and is also unstable to density driven convection in both phases. Observations were made at initial solute concentrations of 0.1 and 0.4 molar. The volume flow rates of alcohol to water were 35/41 $\left[\frac{3.2}{18.2}\right]$ and 50/90 $\left[\frac{4.5}{40.0}\right]$ in ml/min. The pattern was completely unordered at the higher solute concentration due to the highly supercritical conditions.

The dominant pattern at the lower solute concentration is three or four equally spaced straight lines parallel to the flow (see Figure 5). These are indicative of longitudinal roll vortices. The primary difference between this pattern and that observed for pure buoyancy convection is that a fine grain structure is present in this case. In contrast with the large roll structure, these fine scale convective motions were time-dependent. Figure 5 was made at the following conditions: initial solute concentration 0.10 molar, 50 ml/min. alcohol and 90 ml/min. water $\left[\frac{4.5}{40.0}\right]$.

Figure 5 shows four longitudinal lines. These are located, presumably, where the velocity is away from the interface. The fluid moving towards the interface would have the uniform concentration of the bulk and not show up in schlieren pictures. The spacing of these cells is in reasonable agreement with that predicted from linear stability analysis.

DISCUSSION AND CONCLUSIONS

Longitudinal rolls were observed in the experiments under a wide variety of conditions. Rolls were the dominant modes at all conditions for both the pure buoyancy case and the coactive buoyancy surface tension driven case. Rolls were not the dominant mode in the case of confined convection; however, rolls did appear when the volume flow rates were such that the convecting interface region was shifted into a region of greater shear (that is, moved closer to the wall).

The completely unexpected result of the present work was the oscillatory mode observed in confined convection system. The oscillation was clearly a flow induced effect, but we have no mechanism to propose to explain it. Parts I and II solved only the longitudinal and transverse limits and consequently would not predict this intermediate alignment.

The chemical systems considered here have moderate interfacial tensions and relatively high density differences between the two phases. Both Parts I and II would therefore predict the longitudinal mode to dominate the transverse mode. This is verified by experiments. No transverse

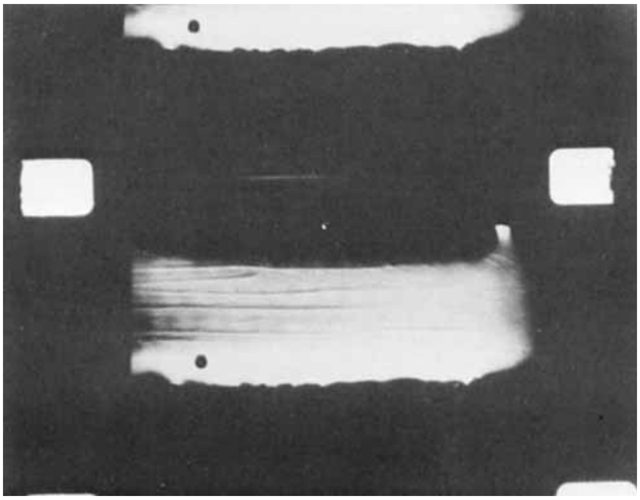

Fig. 4. Typical disturbance structure for buoyancy driven flow. The solvent phases are water and carbon tetrachloride, the former phase at zero net flow and the latter at 18 ml/min., $\left[\frac{0}{12.6}\right]$. The initial solute (acetone) concentration is 0.05 molar in the carbon tetrachloride phase. Note the longitudinal alignment on the left (downstream).

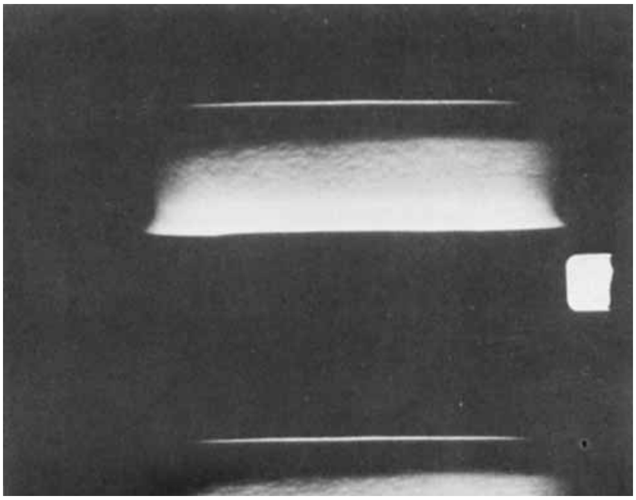

Fig. 5. Typical disturbance structure for surface tension driven flow. The solvent phases are water and carbon tetrachloride, both flowing at 30 ml/min. $\left[\frac{13.4}{21}\right]$. The intial solute (acetone) concentration is 0.20 molar in the water phase. In all pictures the flow is from right to left. The bright bar at the top and dark bar at the bottom are due to the meniscus at the channel walls. A bright diffraction line is visible along one of the channel walls (lower part of picture).

waves were observed.

In closing, it is interesting to note that viscosity stratification induced long waves described by Yih (1967) are not expected for the fluid pairs used here. His analysis for plane Poiseuille flow was extended to show the density difference between the two liquid phases was high enough to stabilize long waves.

LITERATURE CITED

Bakker, C., F. van Vlissingen, and W. Beek, "The Influence of the Driving Force in Liquid-Liquid Extraction—A Study of Mass Transfer With and Without Interfacial Turbulence under Well-Defined Conditions, *Chem. Eng. Sci.*, **22**, 1349 (1967).

Benard, H., and D. Avsec, "Travaux Recents sur les Tourbillons Cellulaires et les Tourbillons en Bandes Applications a L'Astrophysique et a la Metearologie," *J. Phys. Radium*, **9**, 486 (1938).

Berg, J., "Interfacial Phenomena in Fluid Phase Separation Processes" Recent Developments in Separation Science, II," N. Li (ed.), Chemical Rubber Co., Cleveland (1972).

———., A. Acrivos, and M. Boudart, "Natural Convection in Pools of Evaporating Liquids," *J. Fluid Mech.*, **24**, 721 (1966).

Berg, J., and C. Morig, "Density Effects in Interfacial Convection," *Chem. Eng. Sci.*, **24**, 937 (1969).

Brian, P. L. T., and J. Ross, "The Effect of Gibbs Adsorption on Marangoni Instability in Penetration Mass Transfer," *AIChE J.*, **18**, 231 (1972).

Brian, P. L. T., J. Vivian, and S. Mayr, "Cellular Convection in Desorbing Surface Tension-Lowering Solutes from Water," *Ind. Eng. Chem. Fundamentals*, **10**, 75 (1971).

Brunt, D., "Experimental Cloud Formation" in *Compendium of Meteorology*, American Meteorological Soc., Boston (1951).

Chandra, K., "Instability of Fluids Heated from Below," *Proc. Roy. Soc. London*, **164A**, 231 (1938).

Clark, M., and C. King, "Evaporation Rates of Volatile Liquids in a Laminar Flow System," *AIChE J.*, **16**, 64 (1970).

Graham, A., "Shear Patterns in an Unstable Layer of Air," *Phil. Trans. Roy. Soc. London*, **232A**, 285 (1933).

Gumerman, R., and G. Homsy, "Convective Instabilities in Cocurrent Two Phase Flow: Part I. Linear Stability," *AIChE J.*, **20**, 981 (1974).

———., "Convective Instabilities in Cocurrent Two Phase Flow: Part II. Global Stability", *ibid.*

Holder, D., and R. North, "Optical Methods for Examining the Flow in a High Speed Wind Tunnel: Part I Schlieren Methods," NATO AGARDograph 23, 156 (1956).

Linde, H., and E. Schwarz, "Uber groBräumige Rollzellen der freien Grenzflächenkonvecktien," *Mber Akad. Wiss. Berl.*, **6**, 330 (1964).

Maroudas, N., and H. Sawistowski, "Simultaneous Transfer of Two Solutes across Liquid-Liquid Interfaces," *Chem. Eng. Sci.*, **19**, 919 (1964).

Palmer, H., and J. Berg, "Hydrodynamic Stability of Surfactant Solutions Heated from Below," *J. Fluid Mech.*, **51**, 385 (1972).

Phillips, A., and G. Walker, "The Forms of Stratified Clouds," *Quart. J. R. Meteor. Soc.*, **58**, 23 (1932).

Sawistowski, H., "Interfacial Phenomena" in *Recent Advances in Liquid-Liquid Extraction*, C. Hanson (ed.), Pergamon Press, Oxford (9171).

Yih, C., "Instability due to Viscosity Stratification," *J. Fluid Mech.*, **27**, 337 (1967).

Manuscript received August 28 and accepted August 30, 1974.

Mass Transfer in a Fixed-Bed Gas-Liquid Catalytic Reactor with Concurrent Upflow

JAMES W. SNIDER
Oak Ridge National Laboratory
Oak Ridge, Tennessee 37830

and

JOSEPH J. PERONA
Department of Chemical Engineering
University of Tennessee
Knoxville, Tennessee 37916

Mass transfer coefficients for the hydrogenation of α-methylstyrene were measured in a packed-bed reactor with concurrent gas and liquid upflow. The packing was 0.29-cm alumina spheres coated with palladium catalyst. Mass transfer coefficients increased as the ½ power of the liquid rate and increased with gas rate to a gas phase Reynolds number of about 50. The severe decrease for higher gas rates may be due to pulsing flow.

SCOPE

Gas-liquid reactions requiring a solid catalyst are generally carried out in trickle-bed or slurry reactors. Interest in the present system arose during development work at Oak Ridge National Laboratory on a reactor to reduce uranium(VI) to uranium(IV) nitrate in aqueous solution with hydrogen in the presence of a supported palladium catalyst. Higher conversions were obtained with the reactor flooded than in the trickle-bed mode, leading to a study of mass transfer characteristics in concurrent upflow.

The model reaction of hydrogen and α-methylstyrene was chosen because it is a simple reaction with known kinetic rate constants. Furthermore, determination of the degree of conversion is achieved by means of a simple analysis of the product mixture since the only reaction product is cumene. The kinetics of this reaction were studied by Babcock et al. (1957) and Satterfield et al. (1968). The reaction has been used by Satterfield et al.